complex)[32] lies central at $\Delta H^{\ddagger} = 6.3$ kcal mol^{-1} and $\Delta S^{\ddagger} = -19.6$ cal K^{-1} mol^{-1}. Four points are included for metalloprotein–metalloprotein reactions. Sutin, from a similar inspection of a more limited set of data for cytochrome *c* reactions, has suggested that metalloprotein–metalloprotein reactions are associated with more positive $\Delta H^{\ddagger}$ and $\Delta S^{\ddagger}$ values.[38] This point does not appear to be confirmed from the more extensive comparison now possible. Implications of the correlation (and the line drawn) are that $\Delta G^{\ddagger} \sim 12$ kcal mol^{-1}, and the isokinetic temperature is 40 °C.

Since the rate constant k may be regarded as composite ($=Kk_{et}$) whether or not limiting kinetics are observed, it can be presumed that ΔH° and ΔS° are a part of the correlation in Figure 8. A graph of all known ΔH° and ΔS° values (Figure 9) gives an impressive correlation that is according to charge and consistent with ΔH° and ΔS° making major contribution to the separation of points in Figure 8. All the protein reactants in Figure 9 are negatively charged, with complexes 3+ (upper seven points) and 3– (lower points) and the triangle indicating parameters for the association of the 5– complex with cytochrome *f*. We also note that $\Delta H^{\ddagger}$ values for the reactions of plastocyanin, PCu^{I}, and azurin, ACu^{I}, with $[Fe(CN)_6]^{3-}$ and the 5– complex are negative and that the ΔH° component is likely to be negative therefore for these reactions.[27] It is of further interest that three of the points in Figure 9 are for the $[Co(4,7\text{-DPSphen})_3]^{3-}$ complex (4,7-DPSphen = 4,7-bis(phenylsulfonato)phenanthroline), which has a large size and unusual charge distribution. A correlation for $\Delta H_{et}^{\ddagger}$ and $\Delta S_{et}^{\ddagger}$, although giving a similar trend, shows much more scatter.

The correlation in Figure 9 implies a common ΔG° of –4.6 kcal mol^{-1} at a temperature close to 50 °C. On a cautionary note, we should add that although no ΔH° and ΔS° parameters are at present available for 4+ and 5+ complexes, it is unlikely that these will correlate in a similar fashion. Thus, K values for 4+ and 5+ complexes[31] of ~20 000 M^{-1} at 25 °C are unlikely to decrease to around 1000 M^{-1} at 50 °C to conform to the correlation.

Registry No. $[(CN)_5FeCNCo(CN)_5]^{5-}$, 53535-93-6; $[Fe(CN)_6]^{3-}$, 13408-62-3; $[Co(dipic)_2]^{-}$, 71605-21-5; $[Co(bpy)_2(O_2CMe)_2]^{+}$, 16986-92-8; $[Co(phen)_3]^{3+}$, 16788-34-4; $[Zr(C_2O_4)_4]^{4-}$, 21392-82-5; $[Mo(CN)_8]^{4-}$, 17923-49-8; cytochrome *f*, 9035-46-5.

Supplementary Material Available: Listings of rate constants, Tables I–IV and VI–XI (12 pages). Ordering information is given on any current masthead page.

Contribution from the Department of Chemistry, University of Colorado, Boulder, Colorado 80309, and National Bureau of Standards Center for Chemical Engineering, Boulder, Colorado 80303

Selective Transport of Gaseous CO through Liquid Membranes Using an Iron(II) Macrocyclic Complex

C. A. KOVAL,*† R. D. NOBLE,*‡ J. D. WAY,*‡ B. LOUIE,‡ Z. E. REYES,† B. R. BATEMAN,‡ G. M. HORN,‡ and D. L. REED‡

Received September 7, 1984

The equilibrium constant and rate constants for the reversible 1:1 complexation reaction

$$Fe^{II}(TIM)(C_6H_5CN)_2^{2+} + CO \overset{K}{\rightleftharpoons} Fe^{II}(TIM)(C_6H_5CN)(CO)^{2+} + C_6H_5CN$$

have been measured in benzonitrile. At 25 °C, $K_{eq} = K/[C_6H_5CN] = k_1'/k_{-3} = 420$ M^{-1}, $k_1' = 0.14$ M^{-1} s^{-1}, and $k_{-3} = 3.3 \times 10^{-4}$ s^{-1}. In CO-saturated solutions, the Fe(II) complex can be oxidized electrochemically by a $C_rE_rE_rC_i$ mechanism, which allows the diffusion coefficients of the complex and CO adduct to be determined. The reversible complexation reaction of this Fe(II) complex with carbon monoxide affords facilitated transport of CO across benzonitrile liquid membranes. For a membrane with a thickness of 0.072 cm, the transport rate for CO is increased by 14% over the purely diffusional rate. Since the Fe(II) complex does not bind N_2, O_2, CO_2, or H_2, the facilitated transport will be selective for CO in a variety of gaseous matrices. Selectivity is demonstrated for CO/O_2 gas mixtures. The rate constants for CO complexation and the diffusion coefficients for the Fe(II) complexes can be used as input parameters for a mathematical model that predicts the magnitude of the facilitated transport. Furthermore, the model and experimental work indicate that low solubility of the Fe(II) complex limits the magnitude of the facilitated transport in this case, as opposed to the thermodynamics or kinetics of the complexation reaction. The experimental and mathematical procedures described herein can be applied to any 1:1 complexation reaction between a soluble, nonvolatile carrier and a dissolved gas molecule to predict the magnitude of the facilitated transport across liquid membranes.

Introduction

Carbon monoxide is a key raw material in the synthetic routes for a variety of major chemical products including methanol, formaldehyde, acetic acid, isocyanates, aldehydes, formic acid, pesticides, and herbicides. An abundant and relatively inexpensive source of CO would greatly enhance further growth of CO as a raw material for chemical industry. Such growth could result in the CO-based chemical industry approaching the importance of the ethylene-based chemical industry.[1] It is estimated that 1.3×10^{11} kg of CO are released annually from industrial processes in the U.S. as gaseous effluents.[2] These gases can be used as fuel if the concentration of CO is high enough. Much of the dilute CO, however, is flared or discharged with minimum treatment. This unused CO is estimated to exceed 1.8×10^{10} kg (1.5×10^{17} J) per year. Separation and recovery of CO, even a fraction of the total available waste CO, would result in significant improvements via natural-gas displacement.

There are also small-scale requirements for separation and/or detection of CO that are important. Purification of life support system gases in self-contained environments is obviously needed to eliminate the toxic effects of CO on humans. Furthermore, underground mining and workplaces with combustion devices require CO detection and removal.

Rising energy and operating costs have underscored the need for energy-efficient and selective separation processes for gaseous mixtures. A variety of promising separation methods involve reversible chemical complexation, wherein a chemical carrier binds reversibly with the molecule to be separated (permeate).[3-5] One

† University of Colorado.
‡ National Bureau of Standards Center for Chemical Engineering.

(1) Haase, J. M.; Duke, P. M.; Cates, J. W. *Hydrocarbon Process.* **1982**, *61*, 103.
(2) Rohrmann, C. A.; Schiefelbein, G. F.; Molton, P. M.; Li, C. T.; Elliot, D. C.; Baker, E. G. "Chemical Production from Waste Carbon Dioxide-Its Potential for Energy Conservation", BNWL-2137/UC-95F; U.S. DOE: Washington, DC, 1977.

0020-1669/85/1324-1147$01.50/0

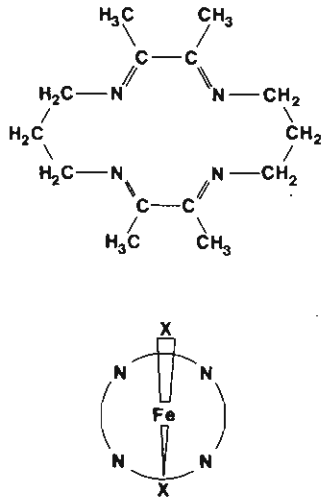

Figure 1. Schematic of TIM molecule and Fe(TIM) with axial ligands attached.

separation method that uses reversible chemical complexation is facilitated transport in liquid membranes. The liquid membrane contains the mobile chemical carrier that remains in the membrane phase. At one interface, the membrane phase contacts the phase that is enriched with the permeate species. The carrier reacts with the permeate to form the complex. The complex diffuses to the opposite boundary where the reverse reaction takes place and frees the permeate into the permeate-lean phase. This method provides a very selective separation while also achieving high flux rates. This method also achieves the separation without the large energy-consuming step of a phase change (i.e., distillation) or a large pressure drop (i.e., polymeric membranes).

The key to developing a separation based on reversible complexation is finding a carrier that binds selectively to the permeate with appropriate equilibrium and rate constants. During the past two decades, there has been considerable interest in the synthesis of molecules capable of selective host–guest reactions that involve organic molecules[6] or metal ions[7,8] as the guest. One important class of hosts includes multidentate macrocyclic compounds. Complexes derived from macrocyclic ligands have been used extensively to model the properties of biological molecules containing transition-metal ions, especially with respect to reversible complexation with dissolved gases such as CO and O_2.[8]

We have used the reversible complexation reaction between CO and the Fe(II) complex derived from the tetraimine macrocyclic ligand 2,3,9,10-tetramethyl-1,3,8,11-tetraazacyclotetradeca-1,3,8,10-tetraene (TIM) to facilitate the transport of CO across membranes constructed from a porous support saturated with benzonitrile (see Figure 1). The complex $Fe^{II}(TIM)(CH_3CN)_2(X)_2$ was first prepared by Baldwin et al.,[9] who demonstrated that the acetonitrile ligands could be replaced by ligands such as imidazole and carbon monoxide. In the case of dissolved CO at ambient pressures, only one of the axial acetonitrile ligands is displaced. The reaction of CO with low-spin Fe(II) complexes in nonaqueous solvents has been examined previously by Vaska and Yamaji[10] and by Stynes and co-workers.[11-13] The thermodynamics and kinetics of reactions involving several $Fe^{II}(TIM)(CO)(X)^{2+}$ complexes have also been studied in aqueous solutions.[14]

Table I. Summary of Physical Constants (C_6H_5CN, 298 K)

Complexation Reaction

$$Fe^{II}(TIM)(C_6H_5CN)_2^{2+} + CO \underset{k_{-3}}{\overset{k_1'}{\rightleftharpoons}} Fe^{II}(TIM)(C_6H_5CN)(CO)^{2+}$$

$k_1' = 0.14\ M^{-1}\ s^{-1}$ $k_{-3} = 3.3 \times 10^{-4}\ s^{-1}$ $K_{eq} = k_1'/k_{-3} = 420\ M^{-1}$

Diffusion Coefficients

$Fe^{II}(TIM)(C_6H_5CN)_2^{2+}$: $2.03 \times 10^{-6}\ cm^2\ s^{-1}$

$Fe^{II}(TIM)(C_6H_5CN)(CO)^{2+}$: $3.11 \times 10^{-6}\ cm^2\ s^{-1}$

Solubilities

CO: 5.5×10^{-3} M (measd, this work)

O_2: 3.8×10^{-3} M (estd, ref 20)

The goal of our research is to develop a procedure whereby fundamental properties of reversible complexation systems can be used to predict facilitated transport. This can be accomplished by using a mathematical analysis developed by Folkner and Noble.[15] We have measured the relevant properties for the $Fe^{II}(TIM)(C_6H_5CN)_2^{2+}/C_6H_5CN/CO$ system and measured the diffusional and facilitated fluxes of CO through a liquid membrane, using a system developed by Bateman et al.[16] The agreement between observed and predicted facilitation is good.

Recently, Kemena et al.[17] developed an optimization model for facilitated transport resulting from reversible chemical complexation. The optimization model allows the chemical factors (reaction rates, diffusion rates, solubility, etc.), which limit facilitated transport for a given system, to be identified. Once these limiting factors are known, facilitation can, in principle, be improved via molecular engineering. In the case of the $Fe^{II}(TIM)(C_6H_5CN)_2^{2+}/C_6H_5CN/CO$ system, the limiting factor is found to be the solubility of the complex in the organic phase.

We believe that the analysis described herein, which relies on measurement of the chemical properties associated with a reversible complexation system, could be applied to a wide variety of separation problems. Carrier systems based on macrocyclic transition-metal complexes seem to be especially promising because the choice of metal atom, oxidation state, and coordination environment can be varied to achieve selectivity for a target permeate and because macrocyclic ligands often afford stable complexes that bind gas molecules in a 1:1 stoichiometry. Finally, a clear understanding of the chemical factors responsible for facilitated transport in synthetic systems should provide insight into related processes in natural systems. The objectives of this study are as follows: first, to report the physical and chemical properties that relate to the reversible reaction between CO and FeTIM; second, to demonstrate that this reaction can be used to facilitate the transport of CO across a liquid membrane; third, to discuss the factors that can lead to increased facilitation of CO.

Experimental Section

Reagents and Materials. The complexes $Fe^{II}TIM(RCN)_2(PF_6)_2$ (R = CH_3, n-C_3H_7, C_6H_5) were prepared by the procedure described by Rose and Reichgott,[18] using the appropriate nitrile solvent diluted 1:10 with ethanol for recrystallization. Recrystallization from butyronitrile gave the highest yield and excellent elemental analysis; therefore, solutions of $Fe^{II}TIM(C_6H_5CN)_2^{2+}$ were prepared from $Fe^{II}TIM(C_3H_7CN)_2(PF_6)_2$ dissolved in benzonitrile. Slight changes in electronic

(3) Schultz, J. S.; Goddard, J. D.; Suchdeo, S. R. *AIChE J. 20*, **1974**, 417.
(4) Kimura, S. G.; Matson, S. L.; Ward, W. J. *Recent Dev. Sep. Sci.* **1979**, *5*, 11.
(5) Way, J. D.; Noble, R. D.; Flynn, T. M.; Sloan, E. D. *J. Membr. Sci.* **1982**, *12*, 239.
(6) Cram, D. J.; Cram, J. M. *Acc. Chem. Res.* **1978**, *11*, 8. Lehn, J. M. *Ibid.* **1978**, *11*, 49. Busch, D. H. *Ibid.* **1978**, *11*, 392.
(7) Izatt, R. M.; Christensen, J. J. "Synthetic Multidentate Macrocyclic Compounds"; Academic Press: New York, 1978.
(8) Smith, P. D.; James, B. R.; Dolphin, D. H. *Coord. Chem. Rev.* **1981**, *39*, 31. Niederhoffer, E. C.; Thomas, J. H.; Martell, A. E. *Chem. Rev.* **1984**, *84*, 137.
(9) Baldwin, D. A.; Pfeiffer, R. M.; Reichgott, D. W.; Rose, N. J. *J. Am. Chem. Soc.* **1973**, *95*, 5152.
(10) Vaska, L.; Yamaji, T. *J. Am. Chem. Soc.* **1971**, *93*, 6673.
(11) Stynes, D. V.; Hui, Y. S.; Chew, V. *Inorg. Chem.* **1982**, *21*, 1222.
(12) Pang, I. W.; Stynes, D. V. *Inorg. Chem.* **1977**, *16*, 590, 2192.
(13) Stynes, D. V.; James, B. R. *J. Am. Chem. Soc.* **1974**, *96*, 2733.
(14) Linck, R. G.; Butler, A. *Inorg. Chem.* **1984**, *23*, 2227.
(15) Folkner, C. A.; Noble, R. D. *J. Membr. Sci.* **1983**, *12*, 289.
(16) Bateman, B. R.; Way, J. D.; Larson, K. M. *Sep. Sci. Tech.* **1984**, *19*, 21.
(17) Kemena, L. L.; Noble, R. D.; Kemp, N. J. *J. Membr. Sci.* **1983**, *15*, 259.
(18) Rose, N. J.; Reichgott, D. W. *J. Am. Chem. Soc.* **1977**, *99*, 1813.

Table II. Transport Measurements

membrane support[a]	dry thickness, cm	liquid membrane thickness, cm	[I], M	N_{CO}[b]	N_{O_2}[b]	F
qual filter paper (2×)	0.034	0.072	0	3.1	3.3	
			0.015	3.9	3.3	1.26
qual filter paper (2×)	0.034	0.072	0	2.7	2.6	
			0.015	2.6	2.4	1.04
qual filter paper (2×)	0.034	0.072	0	2.8	3.0	
			0.015	2.7	2.6	1.11
chromatography paper (1×)	0.034	0.072	0	2.6	2.2	
			0.015	2.7	2.0	1.14
						1.14 ± 0.09 (av)

[a] The filter paper used was Whatman no. 2, which had a particle retention of 8 μm. The chromatography paper used was Whatman 3-mm chromatography paper, which has a water flow rate of 130 mm/30 min. These commercial materials are identified to adequately specify the experimental procedure. Such identification does not imply recommendation or endorsement by the National Bureau of Standards, nor does it imply that the materials or equipment identified are necessarily the best available for this purpose. [b] Fluxes, N, in mol cm^{-2} s^{-1} ($\times 10^{10}$).

spectra indicated that replacement of C_3H_7CN with C_6H_5CN occurs rapidly.

Benzonitrile (99%) was purified by washing with concentrated HCl, drying with K_2CO_3, and vacuum distillation over P_2O_5. Tetrabutylammonium perchlorate (TBAP) was dried in a vacuum desiccator for 12 h prior to use.

Instrumentation. Electronic spectra were recorded on either a Cary 219 spectrophotometer (Certain commercial equipment, instruments, and materials are identified in this paper in order to adequately specify the experimental procedure. Such identification does not imply recommendation or endorsement by the National Bureau of Standards, nor does it imply that the materials or equipment identified are necessarily the best available for that purpose.) or a Hewlett-Packard 8450A diode array spectrophotometer coupled to a flexible disk drive. The Cary 219 instrument is a continuous-beam, scanning UV–vis spectrophotometer while the Hewlett-Packard 8450 is a digital instrument in which short duration pulses of white light pass through the sample several times a second. The absorbance of the sample is determined from the response of an array of photodiodes corresponding to the wavelength range of 200–800 nm. Kinetic experiments were only performed with the Hewlett-Packard 8450 because the complexation rate was photosensitive and the continuous exposure of the sample to light artificially increased the reaction rate. Rotating-disk voltammetry (RDV) was performed with a four-electrode potentiostat, analytical rotator, and speed control. Cyclic voltammetry (CV) was performed with a potentiostat/coulometer and a sawtooth waveform generator. Electrochemical data were recorded on an X-Y recorder or a digital storage oscilloscope.

Electrochemical Measurements. All electrochemical experiments were performed in benzonitrile solutions that were 0.1 M in TBAP. The concentration of electroactive species was ~1 and 2.0 mM in the CV and RDV experiments, respectively. The working electrodes for the RDV and CV experiments were platinum or glassy carbon. Both electrodes were mechanically polished with 0.05-μm alumina prior to use. The compartments of the electrochemical cells that housed the working and reference electrodes were thermostated at 25.0 ± 0.1 °C. The auxiliary electrode was constructed from platinum gauze. For CV experiments, the auxiliary electrode was housed in the thermostated compartment. In the RDV experiments, the auxiliary electrode was placed in a separate compartment that was separated from the thermostated compartment by a sintered-glass frit.

The reference electrode for all electrochemical experiments consisted of a silver wire immersed in a glass tube that was filled with a benzonitrile solution that was 0.01 M in $AgNO_3$ and 0.1 M in TBAP. The end of the tube was sealed with a Vycor frit. All potentials are reported with respect to this reference electrode. The formal reduction potential, E_f, for the ferrocenium/ferrocene couple in benzonitrile was found to be 0.05 V with respect to this reference.[19]

Transport Measurements. The apparatus for the measurement of gas fluxes through immobilized liquid membranes is described elsewhere.[16] Briefly, the apparatus consists of a gas flow system designed to deliver gases at measured flow rates to a membrane cell, the membrane cell, a gas chromatograph with a thermal conductivity detector to determine concentrations of gases leaving the cell, and a computer to record data and permit automated operation of the system.

The column used for separation of CO and O_2 was a 5-ft Carbosieve SII column held at 35 °C. The retention times under these conditions for CO and O_2 were 135 and 85 s, respectively. The system was calibrated by injecting 1.0-cm^3 aliquots of premixed gases (1.0% in N_2) by an automated valve system.

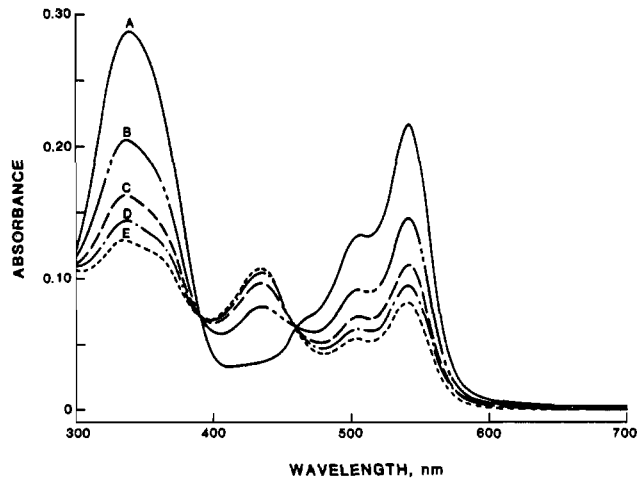

Figure 2. Electronic spectrum of $Fe^{II}(TIM)(C_6H_5CN)_2^{2+}$ (2.0×10^{-4} M) in benzonitrile. Curve A was recorded with no carbon monoxide in solution. Curves B–E represent spectra recorded after I is introduced into a solution that has been saturated with CO.

The liquid membranes consisted of either two thicknesses of qualitative filter paper or one thickness of chromatography paper immersed in benzonitrile solutions for several minutes. Characterization data for the filter and chromatography paper are presented in Table II. The surface area of the membrane was 198 cm^2. The nominal thickness of both liquid membranes was 0.072 cm.

Solubility of Carbon Monoxide in Benzonitrile. Gas chromatography was used to measure the solubility of CO in benzonitrile. Saturated solutions of CO in benzonitrile were prepared by bubbling pure CO through benzonitrile. Incomplete saturation resulted if the CO deaeration periods were shorter than 30 min. The vessel containing the solvent was vented through a syringe needle to prevent air from contacting the liquid and to maintain a constant pressure of CO over the solvent during saturation. Carefully measured samples of the saturated solution were withdrawn with a precision microliter syringe and injected into the gas chromatograph. Comparison of the eluted gas peak with peaks from the calibration runs allowed calculation of the number of moles of CO present in the liquid sample. The concentration of CO in a benzonitrile solution saturated at ambient pressure (83.9 kPa) was calculated to be $(5.5 \pm 0.1) \times 10^{-3}$ M at 25 °C. This value lies between the solubilities reported by Glaldbaek and Andersen[20] for CO in propionitrile and benzyl cyanide of 8.95×10^{-3} and 3.15×10^{-3} M, respectively.

Results

Equilibrium Constant and Rate Constants. In benzonitrile, the $Fe^{II}(TIM)(C_6H_5CN)_2^{2+}$ ion (I) reacts with dissolved carbon monoxide to form the adduct $Fe^{II}(TIM)(C_6H_5CN)(CO)^{2+}$ (II) according to reaction 1. Figure 2 depicts the changes in the

(19) Gagne, R. R.; Koval, C. A.; Lisensky, G. C. *Inorg. Chem.* **1980**, *19*, 2854.

(20) Glaldbaek, J. C.; Andersen, E. K. *Acta Chem. Scand.* **1954**, *8*, 1398.

$$\underset{\text{I}}{Fe^{II}(TIM)(C_6H_5CN)_2^{2+}} + CO \underset{k_{-1}}{\overset{k_1}{\rightleftharpoons}} \underset{\text{II}}{Fe^{II}(TIM)(C_6H_5CN)(CO)^{2+}} + C_6H_5CN \quad (1)$$

UV–vis spectrum for I upon reaction with CO. The bands due to I at 542, 500, and 350 nm decrease in intensity, while a new band appears at 420 nm, which can be attributed to II.[21] Several pieces of evidence indicate that the reaction of I with CO occurs with the simple 1:1 stoichiometry in reaction 1: The isosbestic points at 390 and 450 nm in Figure 1 indicate only two absorbing species in solution. Baldwin et al. were able to isolate the complex $Fe^{II}(TIM)(CH_3CN)(CO)(PF_6)_2$ from acetonitrile solutions of the Fe(II) complex that had been saturated with CO.[9] Data reported herein and by Stynes for acetonitrile solutions[11] indicate that at ambient CO pressures only 20–60% of I is converted into II with no evidence for formation of a dicarbonyl. Other low-spin Fe(II) complexes such as $Fe^{II}(TAAB)(L)_2^{2+}$ and $Fe^{II}(DMGH)_2(L)_2^{2+}$ exhibit 1:1 CO complexation in strong donor solvents such as L = acetonitrile, imidazole, or pyridine.[12]

By treating the concentration of C_6H_5CN in reaction 1 as a constant (9.79 M), the dimensionless equilibrium constant $K = k_1/k_{-1}$ can be rewritten as K_{eq} (M^{-1}) $= K/[C_6H_5CN] = [II]/([I][CO])$. The concentration of I at equilibrium was determined spectrophotometrically by assuming that the absorbance at 542 nm is due entirely to I. A spectrum of $Fe^{II}(TIM)(CH_3CN)(CO)^{2+}$ in acetone reported by Incorvia and Zink reveals that the absorbance of the CO adduct at ~550 nm is <5% of the absorbance at 430 nm.[21] The slight absorbance at ~550 nm could be due to contamination by the bis(acetonitrile) complex. The [I] at equilibrium determined spectrophotometrically is constant for any wavelength between 542 and 570 nm and is quite close to the value determined from rotating-disk voltammetry. A value of K_{eq} = 420 ± 10 M^{-1} at 25 °C was calculated with the [I] at equilibrium, the total concentration of Fe(II), and the solubility of CO in benzonitrile.

The spectral changes depicted in Figure 2 occur when a small [I] is introduced into CO-saturated benzonitrile. A plot of ln ($A_t^{542} - A_{eq}^{542}$) vs. time is linear for more than 4 reaction half-lives. If the absorbance at 542 nm is due to I only, the rate law for this approach to equilibrium is $-d[I]/dt = -dA^{542}/dt = k_{obsd}[I]$. At 25 °C, $k_{obsd} = (1.1 \pm 0.1) \times 10^{-3}$ s^{-1}. On the basis of the kinetic analysis outlined below, k_{obsd} is assumed to be equal to $k_1'[CO] + k_{-3}$ where $k_1'/k_{-3} = K_{eq}$. The rate constants k_1' and k_{-3} are used to calculate the facilitated flux of CO across membranes containing I.

Kinetic studies of the reversible binding of CO to $Fe^{II}(TIM)(RCN)_2^{2+}$ and other low-spin Fe(II) complexes are consistent with the following mechanism:[10,12]

$$Fe^{II}(TIM)(RCN)_2^{2+} \underset{k_{-2}}{\overset{k_2}{\rightleftharpoons}} Fe^{II}(TIM)(RCN)^{2+} + RCN \quad (2)$$

$$Fe^{II}(TIM)(RCN)^{2+} + CO \underset{k_{-3}}{\overset{k_3}{\rightleftharpoons}} Fe^{II}(TIM)(RCN)(CO)^{2+} \quad (3)$$

Application of the steady-state approximation to $Fe^{II}(TIM)(RCN)^{2+}$ predicts that the rate law for the approach to equilibrium from left to right in reaction 1 would be

$$-\frac{d[I]}{dt} = \frac{k_2k_3[I][CO] - k_{-2}k_{-3}[II][C_6H_5CN]}{k_{-2}[C_6H_5CN] + k_3[CO]}$$

Previous studies have shown that the rate constants for the reaction of $Fe^{II}(TIM)(RCN)^{2+}$ with RCN and CO, k_{-2} and k_3, are within a factor of 10 of each other.[10-13] Since under our reaction conditions [RCN] ~2000[CO] and $k_{-2}[C_6H_5CN] \gg k_3[CO]$, the rate law reduces to

$$-\frac{d[I]}{dt} = \frac{k_2k_3}{k_{-2}[C_6H_5CN]}[I][CO] - k_{-3}[II] = k_1'[I][CO] - k_{-3}[II]$$

(21) Incorvia, J. J.; Zink, J. F. *Inorg. Chem.* **1977**, *16*, 3161.

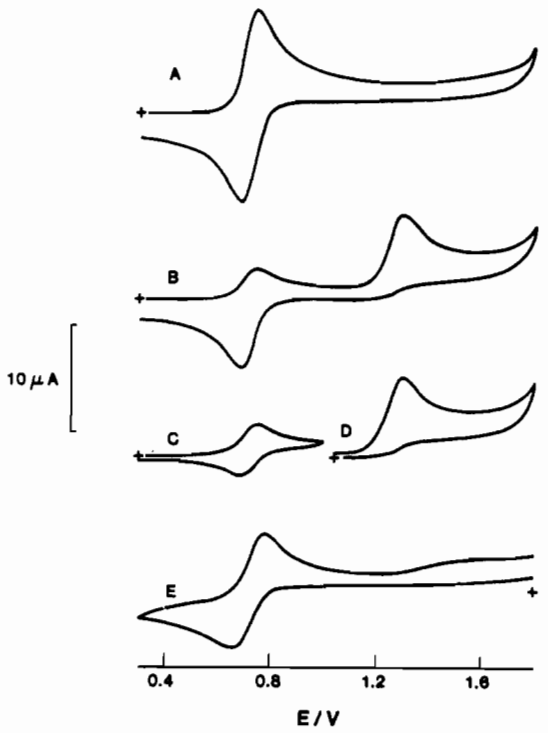

Figure 3. Cyclic voltammograms of $Fe^{II}(TIM)(C_6H_5CN)_2^{2+}$ (1.4×10^{-3} M) at glassy carbon in benzonitrile with 0.1 M TBAP. Scan rate is 50 mV s^{-1}. Curve A was recorded with solution purged with N_2. Curves B–E were recorded with solution purged with CO.

By noting that $[I]_{eq} + [II]_{eq} = [I] + [II]$ and $k_1'/k_{-3} = K_{eq} = [II]_{eq}/([I]_{eq}[CO])$, the rate law for approach to equilibrium simplifies to

$$-\frac{d[I]}{dt} = (k_1'[CO] + k_{-3})([I] - [I]_{eq})^{22}$$

Assuming $k_{obsd} = k_1'[CO] + k_{-3}$, values of k_1' and k_{-3} are calculated to be 0.14 M^{-1} s^{-1} and 3.3×10^{-4} s^{-1}, respectively. The values of K_{eq} and k_{-3} are in reasonable agreement with values reported by Stynes for acetonitrile solutions.[11]

Reaction with Other Gas Molecules. Solutions of I in benzonitrile were purged with H_2, CO_2, O_2, and N_2 for at least 30 min. No changes in the electronic spectra of I were observed, indicating that these dissolved gases do not form complexes with I in benzonitrile at ambient pressures.

Cyclic Voltammetry of Complexes I and II. Electrochemical oxidation of I and II provides a method for the determination of the diffusion coefficients, D_r, of these species and provides certain checks on the equilibrium and rate constants obtained spectrophotometrically. Figure 3 contains cyclic voltammograms of I in benzonitrile saturated with N_2 (curve A) and CO (curves B–E). The wave in curve A represents the 1e, reversible oxidation of I to $Fe^{III}(TIM)(C_6H_5CN)_2^{3+}$ (III). The peak separation ΔE_p is close to the theoretical value of 58 mV and is nearly independent of scan rate.[23] The unity n value was confirmed by constant-potential electrolysis. The formal reduction potential of the process III + e^- = I was calculated from $(E_{p,a} + E_{p,c})/2$ and found to be 0.700 ± .005 V.

If the solution from which curve A was obtained is saturated with CO, the anodic peak current, $i_{p,a}$, for the wave at 0.7 V is reduced in size and a new irreversible wave appears with $E_{p,a}$ = 1.35 V (curve B). Also, the cathodic peak current, $i_{p,c}$, for the wave at 0.7 V becomes larger than $i_{p,a}$. Curve C shows that, if the scan is reversed at 1.05 V, $i_{p,a}$ is equal to $i_{p,c}$ as in curve A. Curve D shows that the position and size of the irreversible wave

(22) Espenson, J. H. "Chemical Kinetics and Reaction Mechanisms"; McGraw-Hill: New York, 1981; pp 42–48.
(23) Bard, A. J.; Faulkner, L. R. "Electrochemical Methods"; Wiley: New York, 1980; pp 227–230.

Scheme I

$$Fe^{II}(TIM)(C_6H_5CN)_2^{2+}\ (I) + CO \overset{K_{eq}}{\rightleftharpoons} Fe^{II}(TIM)(C_6H_5CN)(CO)^{2+}\ (II)$$

$$I \rightleftharpoons Fe^{III}(TIM)(C_6H_5CN)_2^{3+}\ (III) + e^- \qquad E_f(1) = 0.700\ V$$

$$II \rightleftharpoons Fe^{III}(TIM)(C_6H_5CN)(CO)^{3+}\ (IV) + e^- \qquad E_f(2) = >1.5\ V$$

$$IV + C_6H_5CN \longrightarrow III + CO \qquad k_d^{III}$$

is independent of initial potential.

The electrochemical behavior of I is consistent with the reactions depicted in Scheme I. If only the wave at 0.7 V is scanned (curve C), the reduction of size from curve A is consistent with C_rE_r mechanism in the pure diffusion region;[24,25] i.e., the kinetics of the reversible reaction with CO are too slow to be manifested in the oxidation of I, and II cannot be oxidized at the potentials in curve C. At the concentration of iron complex used in preparing Figure 2 (1.4 mM), the spectrophotometrically determined value of K_{eq} predicts that in a CO-saturated solution the [I] = 4.2×10^{-4} M and the [II] = 9.8×10^{-4} M. Since [CO] = 5.5×10^{-3} M, the system can be viewed as a pseudo-first-order equilibrium

$$I \underset{k_{-3}}{\overset{k_1''}{\rightleftharpoons}} II \qquad (4)$$

where $K_{eq}' = K_{eq}[CO] = 2.31$ and $k_1'' = k_1'[CO] = 7.7 \times 10^{-4}$ s^{-1}. By use of the reaction zone diagram developed by Saveant and Vianello[25] with the dimensionless kinetic parameter λ equal to $(RT/F)(k_1'' + k_{-3})/v$, it can be shown that v must be less than 3×10^{-4} V s^{-1} in order for the CO-complexation reaction to be manifested in curve C.

Comparison of $i_{p,a}$ in curves A and C allows the calculation of $K_{eq}' = (i_{p,a}(N_2)/i_{p,a}(CO)) - 1 = 2.6$. The slight difference between the spectrophotometrically and electrochemically determined values of K_{eq}' could be due to the effect of supporting electrolyte on the solubility of CO, the thermodynamics of reaction 1, or the fact that reaction 4 is not a true first-order equilibrium.

The irreversible wave in curves B and D can be attributed to the oxidation of II to $Fe^{III}(TIM)(C_6H_5CN)(CO)^{3+}$ (IV) followed by the rapid loss of CO from IV to form III, i.e., by an E_rC_i (or E_qC_i) mechanism.[26] Accurate voltammetric data for the irreversible wave can be obtained by using 0.8 V as the initial potential as in curve D. Even though the diffusion layer contains no I at this potential, the concentration of II is unaffected because the half-life for the dissociation of CO from II is nearly 30 min. Cyclic voltammetry of the irreversible wave was recorded for scan rates between 0.020 and 1.0 V s^{-1}. The wave remained irreversible at all scan rates. A plot of $i_{p,a}$ vs. $v^{1/2}$ was nearly linear but with slight downward curvature as is predicted for a E_rC_i mechanism in the purely kinetic region.[25] Furthermore, values of $E_{p,a}$ for the wave in curve D shift positive with increasing scan rate. This shift is greater than the theoretical value for an irreversible wave of 30 mV/decade,[26] probably due to uncompensated resistance in the cell or slow heterogeneous charge-transfer kinetics. If the mechanism in the scheme is correct, E_f for the oxidation of II to IV must be $>\sim 1.5$ V and k_d^{III} must be $>\sim 200$ s^{-1}.

The increased magnitude of $i_{p,c}$ for the wave at 0.7 V in curve B can also be explained by Scheme I. When II is oxidized to IV and rapidly releases CO to give III, the diffusion layer has a concentration of III that is greater than the concentration due to the oxidation of I. The necessity of scanning through the irreversible wave in order to obtain the increased cathodic peak current is evident from curves B and C in Figure 2. The magnitude of $i_{p,c}$ in curve B was not analyzed mathematically; however, a voltammogram recorded with $E_i = 1.8$ and 0.3 V as the switching potential (curve E) has a wave at 0.700 V that is larger than the wave in curve B, and the irreversible wave at 1.4 V has almost disappeared. This result is obtained because at 1.8 V the diffusion layer consists almost entirely of III.

Diffusion Coefficients Using Rotating-Disk Voltammetry. When I is oxidized at a platinum rotating-disk electrode, the behavior observed is similar to the cyclic voltammetric behavior. In N_2-saturated solutions, a single oxidation wave is observed with $E_{1/2} = 0.700$ V. This wave is reversible as established from plots of $i_{l,a}$ vs. $\omega^{1/2}$ and E vs. log $(i_{l,a} - i)/i$ where $i_{l,a}$ is the limiting anodic current and ω is the rotation rate. In CO-saturated solutions, the wave at 0.7 V is diminished in size and a new wave appears with $E_{1/2} \simeq 1.4$ V. Comparison of the limiting currents for the wave at 0.7 V under N_2 and CO allows K_{eq}' to be calculated from $K_{eq}' = (i_{l,a}(N_2)/i_{l,a}(CO)) - 1$ and is equal to 2.4. This value is probably more accurate than the value determined from cyclic voltammetry because limiting currents are more easily measured than are peak currents.

The diffusion coefficient of I was calculated by the Levich equation[27] from limiting currents obtained under N_2 and found to be $(2.03 \pm 0.05) \times 10^{-6}$ cm^2 s^{-1}. The diffusion coefficient of II was calculated similarly from the limiting current for the wave at ~ 1.4 V and found to be $(3.11 \pm 0.05) \times 10^{-6}$ cm^2 s^{-1}. The [II] was calculated from the difference between the total concentration of complex and the [I] present in a CO-saturated solution. The fact that D_{II} is greater than D_I is expected because CO is a smaller ligand than is C_6H_5CN.

Summary of Physical Constants. Table I contains the physical parameters of the $Fe^{II}(TIM)(C_6H_5CN)_2^{2+}/C_6H_5CN/CO$ systems that are relevant to the transport of gaseous CO across liquid membranes.

Transport of CO and O_2 across Liquid Membranes. The effect of $Fe^{II}(TIM)(C_6H_5CN)_2^{2+}$ on the transport of CO across liquid membranes was determined utilizing gaseous mixtures of CO and O_2 in roughly a 1:1 molar ratio. Since O_2 was shown not to form complexes with I, the effect of I on the transport of O_2 was assumed to be negligible. The use of a gas mixture containing a complexing and a noncomplexing permeate gas is preferable to single-component measurements, because systematic errors due to changes in operation conditions are readily detected.

Representative data for a series of transport experiments are contained in Table II. Each experiment consists of flux measurements for CO and O_2 in the absence and presence of I, N^D and N^F, but with identical flow conditions. The fluxes are steady-state values that are achieved after ~ 30 min and remain constant for 30–60 min. By assuming that the facilitation factor for O_2 is unity, i.e., $N_{O_2}{}^D = N_{O_2}{}^F$ for identical flow conditions, a value of F for CO that is corrected for variations in O_2 flux can be calculated as

$$F_{CO} = (N^F{}_{CO}/N^F{}_{O_2})(N^D{}_{O_2}/N^D{}_{CO})$$

These values of F_{CO} are included in Table II and average 1.14 ± 0.09.

Comparison of the average diffusional flux for CO, 2.8×10^{-10} mol cm^{-2} s^{-1} with the value calculated from Fick's law, 5.4×10^{-10} mol cm^{-2} s^{-1}, indicates that the effective diffusion length for the materials used in this work is approximately twice the nominal length or 0.14 cm.

Discussion

Comparison of Theoretical and Experimental Results. A schematic representation of a facilitated-transport liquid membrane is shown in Figure 4. In the absence of carrier I, the fluxes of CO and O_2, N_{CO} and N_{O_2}, across the liquid membrane can be calculated from Fick's law, the effective membrane thickness L, the solubilities of CO and O_2 in the liquids and their partial pressures in the permeate-rich phase, and the diffusion coefficients of CO and O_2 in the liquid, D_{CO} and D_{O_2}. The effective membrane thickness accounts for tortuosity in the diffusion length imposed by the solid support for the liquid as well as mass transport resistances at each interface.

In the absence of carrier, the concentration profiles for CO and O_2 are linear and the flux is directly proportional to the slope of

(24) Reference 23, pp 443–445.
(25) Saveant, J. M.; Vianello, E. *Electrochim. Acta* **1963**, *8*, 905.
(26) Reference 23, pp 437–442, 451–455.
(27) Reference 23, pp 286–290.

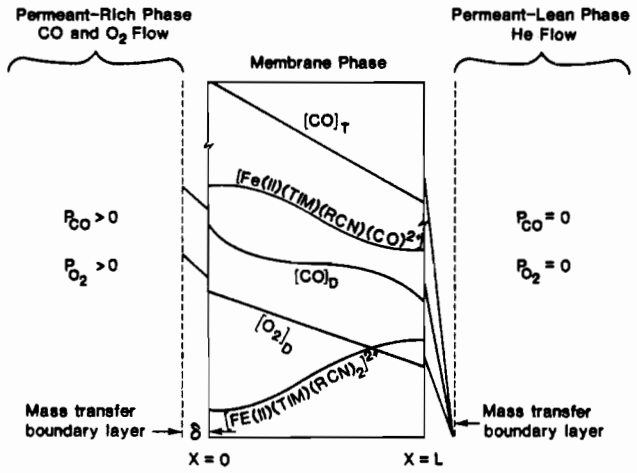

Figure 4. Schematic representation of steady-state concentration profiles for CO and O_2 transport through an immobilized liquid membrane containing $Fe^{II}(TIM)(RCN)_2^{2+}$ as a carrier. Distance in the vertical direction represents concentration; however, the drawing is not to scale.

the profile. As indicated in Figure 4, the presence of $Fe^{II}(TIM)(RCN)_2^{2+}$ in the membrane causes the predicted concentration profile for CO but not for O_2 to be altered. The profile for total CO is the sum of the profiles for dissolved CO and for $Fe^{II}(TIM)(RCN)(CO)^{2+}$ and will have a slope that is greater than or equal to the slope of the profile for CO in the absence of carrier. This leads to facilitation factors for CO that are ≥ 1.0.

The facilitation factor for the $Fe^{II}(TIM)(C_6H_5CN)_2^{2+}/C_6H_5CN/CO$ system was calculated from the rate constants k_1' and k_{-3}, L, the diffusion coefficients D_I and D_{II}, the total concentration of carrier $[Fe^{II}]_T = [I] + [II]$, and the concentration of permeate at $x = 0$, $[CO]_{x=0}$ (see Figure 4). This calculation was done by using the model of Folkner and Noble.[15] The computation is simplified by expressing these parameters as three dimensionless variables:

$$K_d = k_1'[CO]_{x=0}/k_{-3} = [II]/[I] =$$
dimensionless equilibrium constant

$$\epsilon = D_{II}/k_{-3}L^2 =$$
ratio of characteristic reaction to diffusion times

$$\alpha = (D_{II}/D_{CO})([Fe^{II}]_T/[CO]_{x=0}) =$$
mobility ratio of carrier to solute

Kemena et al.[17] provide working curves that allow the maximum F to be estimated for certain situations and depict the interplay between the three variables.

With the model of Folkner and Noble,[15] and if the effective membrane thickness is used, the calculated steady-state value of F for CO is 1.12. The agreement between this calculated value and the average experimental value of 1.14 is remarkable considering the experimental difficulty associated with measuring F values that are slightly greater than unity.

Use of I and Other Macrocyclic Complexes as Carriers. In general, complexes derived from macrocyclic or other multidentate ligands have several properties that are advantageous for studying facilitated transport. Achieving 1:1 reaction stoichiometry is important because it provides a system in which all the relevant properties are measurable and the modeling mathematics are tractable. Since multidentate ligands occupy many of the available coordination sites around the metal and since the substitution kinetics of multidentate ligands are often sluggish, simple 1:1 reactions with other monodentate ligands are common and easily studied. Furthermore, multidentate ligands often stabilize the metal atom toward other irreversible reactions that would otherwise compete with complexation.

One of the most useful features of the working curves provided by Kemena et al.[17] is the ability to compare the properties of a real carrier/permeate system with the properties of an optimal system. This analysis often suggests ways that the carrier can be modified to achieve better facilitated transport. The I/CO system meets one crucial criteria in that it is selective for CO. Obviously, the requirements for selectivity are dependent on the other species in the permeate-rich phase. The complications that will arise if the carrier binds to several species in a mixture are easily envisioned.

Besides selectivity, the most important property for facilitation is the magnitude of the equilibrium constant of the complexation reaction with respect to the concentration of permeate. The dimensionless variable reflecting these effects is K_d. Kemena et al. show that for most situations the optimal value of K_d is between 1 and 10. For gaseous permeates with solubilities around 5×10^{-3} M and partial pressures from 1.01×10^4 to 1.01×10^5 Pa, this corresponds to values of K_{eq} = [complex]/([free carrier]-[permeate]) between 2×10^2 and 2×10^4 M^{-1}. The value of K_{eq} for the complexation of I with CO of 420 M^{-1} falls toward the lower end of this range. It should be emphasized that strong binding of the permeate to the carrier, $K_{eq} > 10^5$ M^{-1}, is not desirable because the kinetics for release of the permeate will be too slow. The fact that relatively weak complexation is required for high facilitation makes it somewhat easier to choose a carrier with the proper selectivity. The complex I in nitrile solvents is "selective" for CO simply because it does not bind to weaker field ligands.

If K_d has an appropriate value, the second most important factor is the inverse Damkohler number ϵ, which is the ratio of diffusion to reverse reaction rate. In general, smaller values of ϵ lead to larger facilitation factors. The most effective way to decrease ϵ is to have rapid complexation kinetics. In the case discussed here, the kinetics are controlled by the substitution kinetics of low-spin, d^6 Fe(II), which tend to be relatively slow. The value of ϵ for this system is about 0.5, and for 1.01×10^5 Pa of CO the value of K_d is 2.3. These values do not preclude high facilitation factors; indeed, F could be as high as 3–4 if α was as high as 50. Due to the limited solubility of I in benzonitrile, α is on the order of 2–5. If $\alpha < 1$, F will be <2 regardless of the values of ϵ and K_d (see Figure 4 in ref 17). The most straightforward way to increase F for this system is to synthesize derivatives of TIM that lead to more soluble Fe(II) complexes.

Acknowledgment. Z.E.R. was supported by a fellowship from the University of Puerto Rico.

Registry No. C_6H_5CN, 100-47-0; CO, 630-08-0; Fe, 7439-89-6.